Catalysis Today 143 (2009) 347–354

Contents lists available at ScienceDirect

Catalysis Today

journal homepage: www.elsevier.com/locate/cattod

Wetting angles and photocatalytic activities of illuminated TiO_2 thin films

V. Rico, P. Romero, J.L. Hueso, J.P. Espinós, A.R. González-Elipe *

Instituto de Ciencia de Materiales de Sevilla (CSIC-Univ. Sevilla), Avda. Américo Vespucio 49, 41092 Sevilla, Spain

ARTICLE INFO

Article history:
Available online 26 November 2008

Keywords:
TiO_2
Photo-catalytic activity
Wetting angle
Thin films

ABSTRACT

TiO_2 thin films have been prepared by physical vapour deposition (PVD) and plasma enhanced chemical vapour deposition (PECVD) to study the UV-induced photo-activity of this material. Wetting angle variations and photo-catalytic activity for the degradation of dyes upon UV illumination have been compared for thin films with different crystalline structure (amorphous, rutile and anatase), microstructure (columnar, compact, etc.) and porosities as estimated from the values of their refraction indices and their direct assessment with a quartz crystal monitor. The surface of the thin films became superhydrophilic upon UV light irradiation and then it recovered its original state by keeping the samples in the dark. Wetting angle decays follow very similar kinetics for amorphous and crystalline films, independently of their actual porosities. By contrast the photo-catalytic activity was very dependent on the crystalline structure of the films (anatase > rutile > amorphous) and on their porosities. The different behaviour depicted by the films with regard to these two properties suggests that they respond to different though related mechanisms and that they cannot be considered as equivalent when trying to prove the photo-activity of TiO_2.

1. Introduction

Since the discovery by Wang et al. [1] that the surface of TiO_2 becomes superhydrophilic (i.e., wetting angle smaller than 10°) when it is illuminated with UV light, this property has been generally associated with the well known and widely studied photo-catalytic activity of this material [2,3]. Thus, many works on this subject have implicitly assumed that both photo-catalytic activity and light-induced hydrophilicity are expression of the same type of basic processes and that, therefore, they give account on the same type of properties [2,4,5]. Very likely, this belief is supported by the absence of systematic studies where these two properties are compared for series of TiO_2 thin films with different structural and microstructural characteristics.

In the present paper we have compared the photo-catalytic activity and the wetting behaviour of two series of TiO_2 thin films prepared by plasma enhanced chemical vapour deposition (PECVD) and by physical vapour deposition (PVD). Depending on the preparation parameters and thermal post-treatments, films with different crystal structure (anatase, rutile, amorphous), porosity and microstructure have been prepared. The efficiency of these thin films towards the photo-degradation of dyes in aqueous solutions and the kinetics of transformation of the wetting angle from partially hydrophobic into superhydrophilic (i.e., wetting angles smaller than 10°) are critically compared. In the frame of this comparative study, it also arose the question of the influence of the structure and porosity of the films on their photo-activity.

For TiO_2 in the form of powders this type of correlations has been widely studied [6–8] and it is now clear that, for example, the anatase structure or the surface area of fine divided solids are critical to maximize the photo-activity of this material. Similar studies are scarcer for TiO_2 in the form of thin films [9,10], where concepts like microstructure or porosity are more elusive and difficult to quantify. Therefore, a second objective of the present work is trying to ascertain the influence of these thin film characteristics on the photo-activity of this material. For this purpose, we have changed the experimental protocols of preparation by PVD and PECVD in order to get thin films with different porosities, microstructures and crystalline structures. The obtained results have provided some hints to account for the influence of the microstructure and other morphological characteristics of the films on their photo-catalytic activity and their ability to transform their surfaces into superhydrophilic when they irradiated with UV light.

* Corresponding author. Tel.: +34 954489528; fax: +34 954460665.
E-mail address: arge@icmse.csic.es (A.R. González-Elipe).
URL: http://www.sincaf-icmse.es/

0920-5861/$ – see front matter © 2008 Published by Elsevier B.V.
doi:10.1016/j.cattod.2008.09.037

2. Experimental

2.1. Materials

2.1.1. TiO_2 thin films prepared by PECVD

TiO_2 thin films with a thickness between 300 and 500 nm were prepared by PECVD in a plasma reactor with a remote configuration. The substrates, consisting of pieces of a silicon wafer or transparent silica plates, were kept at room temperature or at 250 °C during the preparation of the films. The plasma system, supplied with a microwave (MW) plasma source (SLAN, from Plasma Consult, GMbh, Germany), has been described in a previous work [11]. It consists of an external MW source (i.e., downstream configuration) coupled to the reaction chamber and separated from it by a grounded grid to avoid the microwave heating of the substrates. Distance from substrate and grid was 10 cm. This grid also minimizes the concentration of ionic species in the deposition zone where the substrate and the precursor dispenser are located. These conditions contribute to minimize ion bombardment effects on the substrate. Measurements about the distribution of ions, electrons, and neutral species below and above the grid can be found in Ref. [12]. The source was operated with a power of 400 W with pure O_2 as plasma gas. The synthesis of the films was carried out at room temperature and 250 °C as temperatures of the substrate. Titanium tetrakis isopropoxide (TTIP) was used as titanium precursor. For dosing the TTIP in a controlled way it was placed in a stainless steel receptacle through which oxygen was bubbled while heating at 40 °C. Both the bubbling line and the shower-type dispenser used to dose the precursor into the chamber were heated at 100 °C to prevent any condensation in the tube walls. Total pressure during deposition was 5.1×10^{-1} Pa at normal operation conditions. These samples will be labelled in the text as PECVD-*t*, where *t* refers to the temperature of the substrate during the preparation.

Thin films of the type PECVD-250 were annealed in air in a furnace at 1150 °C for 3 h to get a thin film with the rutile structure. In the text this thin film is labelled as PECVD-1150 (R).

2.1.2. TiO_2 thin films prepared by PVD

TiO_2 thin films with a thickness ranging from 300 to 500 nm were prepared by PVD in an electron evaporation system. TiO_2 pellets were used as material for evaporation. To get fully stoichiometric thin films a constant oxygen partial pressure ($P \sim 10^{-1}$ Pa) was maintained in the chamber during evaporation. The substrates, consisting of pieces of a silicon wafer or transparent silica plates, were kept at room temperature or at 400 °C during the preparation of the films. To control the porosity and the surface roughness, evaporation was carried out at different glancing angles with respect to the evaporation source. This geometry leads to columnar microstructures with much porosity and high surface roughness [13,14]. All the samples considered here were prepared for the same period of time under similar preparation conditions with an approximate growing rate at normal incidence of 6 nm min^{-1}. Because of the geometric conditions of evaporation, the thickness of the films prepared at glancing angles (i.e., 85°) was smaller than that of those prepared at normal evaporation. The PVD samples will be labelled in the text as PVD-*t*, where *t* refers to the temperature of the substrate during the preparation. When the samples were prepared at a glancing geometry the thin films are named as PVD-*t* (G).

Another type of film was prepared by e-beam evaporation at normal geometry and 400 °C as temperature of the substrate while their growth was assisted by low energy (600 eV) O_2^+ ion bombardment (ion beam assisted deposition, IBAD [15]) with a beam current of 3 μA (approximately an ion/atom ratio of 0.1). The ion gun utilized was supplied by Plasma Consult (IQP model). These samples are labelled in the text as PVD-400/O_2^+.

2.2. Methods

The crystalline structure of the films was assessed by X-ray diffraction in a Siemens D5000 Spectrometer working in the Bragg-Brentano configuration and using the Cu Kα radiation as excitation source.

The microstructure of the films was assessed by scanning electron spectroscopy (SEM). Normal and cross-sections views were taken for thin films grown on silicon on a Hitachi S5200 field emission microscope working at 5.0 keV. To get the cross-section views of the films, the silicon wafers with the films of their surface were broken up through a mark made with a diamond tip.

Illumination of the samples for contact angle measurements was carried out with a Xe lamp with a photon intensity at the position of the samples of 2 W cm^{-2} for the complete UV + vis spectrum of the lamp. From this intensity a power of ca. 0.4 cm^{-2} corresponded to photons with $\lambda < 380$ nm. For simplicity we will refer this situation in the text and figures as UV illumination. In all cases an infrared filter (i.e., a water bath) was kept between the lamp and the samples to remove the IR photons and thus prevent any possible heating by the infrared radiation.

Measurement of contact angle was carried out by the Young method by dosing small droplets of deionized and bidistilled water on the surface of the illuminated samples. In the experiments where the contact angle variation was determined as a function of the illumination time, a metal foil acting as a shutter was used to close and open the lamp output. All wetting angle measurements within a given experiment were taken after illumination for successive periods of time. Therefore, the time scale in the plots refers to the accumulative illumination of the samples. The uncertainty in the determination of the water contact angle is about 5° depending on the sample position. In the course of this investigation it was noticed that, in general, the "as-prepared" thin films were more hydrophilic than the same samples a given time after their preparation. Therefore, storage conditions were carefully controlled by putting the samples in a desiccator before their use. The reported experiments were carried out with samples that have been stored for a sufficiently long period of time, so that they had stabilized their surface properties (minimum of 2 months after their preparation).

Photocatalytic tests were carried out in a specially constructed experimental set-up. It consisted of a small cell made of quartz (total volume 3 cm^3) where 2 cm^3 of a 3.5e−5 M solution of methyl orange dye was placed together with a piece of a silicon substrate (1×0.8 cm^2) with the thin film deposited on its surface. The film was irradiated from a frontal position while simultaneously spectra of the solution were recorded with the help of two optical fibres connected to a UV–visible spectrometer and placed in opposite sides of the vessel. The solution was bubbled with oxygen and the vessel closed with a Teflon cover to avoid the evaporation of the liquid. The whole set-up was refrigerated with a fan placed behind the vessel. This experimental set-up permitted the automatic recording of the spectra from the solution while the films are irradiated. Reference experiments were also carried out with the solution without the thin films to detect the decay of the dye concentration as a result of its irradiation with UV light. The intensity of the UV + vis radiation at the position of the cell was 1.8 W (i.e., approximately 0.3 W cm^{-2} for photons with $\lambda < 380$ nm). Since the illumination area of the samples was defined with a slit of 1 cm^2 and was always the same for all the experiments, their results can be properly compared. This is not always the case with dye degradation experiments carried out

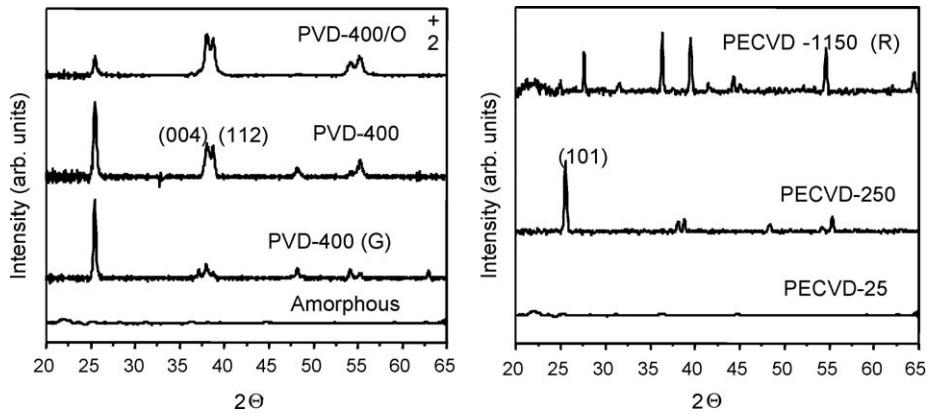

Fig. 1. XRD diagrams of the thin films prepared by PVD (left) and PECVD (right). All the amorphous films depicted a similar flat line as indicated. Peaks corresponding to crystal planes presenting a preferential growth parallel to the surface are indicated.

with powders or pellets, where a different agglomeration of the particles may produce inconsistencies and reproducibility problems.

Provided that the thin films do not scatter the light, a way of estimating their porosity is by measuring their refraction indices [16]. Values of refraction indices of the films were obtained from their UV–vis transmission spectra when they were supported on a quartz plate. These spectra were recorded with a Perkin-Elmer Lambda 12 spectrometer in transmission mode using conventional optical methods to reproduce their shape. For given samples, the obtained values of refraction index have been compared with their actual total porosity expressed in terms of percentage of void volume determined from the analysis of water adsorption isotherms obtained with the help of a quartz crystal monitor (QCM) [17]. Since a heating treatment of the thin films/QCM specimen may degrade the adhesion of the films or contaminate them, porosity data are only provided for thin films prepared at room temperature and 250 °C. Note that for supported thin films with a thickness of the order of some hundreds of nanometer, the classical BET methods cannot be used because lack of sensitivity and the instrumental restriction that the films are supported on substrates made of glass, quartz or another rigid material.

3. Results

3.1. Characterization of the TiO_2 thin films

The structure of the films was determined by XRD. The diagrams of the films are shown in Fig. 1 and the corresponding structures reported in Table 1. While the films prepared at room temperature were amorphous, those prepared at 250 °C by PECVD and 400 °C by PVD presented the anatase structure. A PECVD-250 film annealed at 1150 °C depicted the rutile structure. Besides this basic assessment of the structure of the thin films, the diagrams in Fig. 1 also show that their texture was different. Thus, samples PVD-400, PVD-400 (G) and PVD-400/O_2^+ depict a preferential growth of the (0 0 4) and (1 1 2) crystal planes, while for sample PECVD-250, a preferential growth of the (1 0 1) plane parallel to the sample was found.

The control of the deposition conditions by either PECVD or PVD has allowed us to get thin films where not only the crystallographic structure but also the microstructure and porosity are controlled. Normal and cross-section views of the different samples are shown in Figs. 2 and 3. From these micrographs the main microstructural characteristics of the different thin films have been summarized in Table 1. Due to charging effects no clear SEM micrographs were obtained for the PECVD-1150 (R) sample, particularly for its cross-section view. This was likely due to the fact that the surface of the silicon substrate was also oxidized after the heating treatment thus degrading the electrical contact of the sample with the microscope holder. It is particularly interesting that all the films present a columnar microstructure and that for the PVD films prepared at a glancing geometry the columns are tilted and leave open a large space between them. This microstructure is typical of thin films prepared by PVD at glancing geometries [13,14]. It is also noticeable that in sample PECVD-250 small crystallites can be clearly distinguished in both the cross-section and the normal views.

UV–vis transmission spectra of the different films are shown in Fig. 4. It can be observed that the PECVD-1150 (R) sample disperses the light as deduced from the lower transmittance of this sample and the distorted shape of its spectrum with respect to that of a transparent sample. For this situation the common models used to extract the refraction indices from the oscillations of the transmission spectra cannot be used and therefore no information about refraction index is available in this case [16,18]. Fig. 4 also shows that the amplitude of the oscillations in the transmission spectra is quite different depending on the thin film. These oscillations are the result of the interference of the light beams reflected at the external surface of the films and at the substrate/

Table 1
Main characteristics of the thin films used in the present work.

Sample	Refraction index	Porosity (% of void volume)	Structure	Microstructure
PVD-400	2.32	–	Anatase	Compact columns
PVD-25	2.27	8.3	Amorphous	Compact columns
PVD-400 (G)	1.72	–	Anatase	Separate and tilted columns
PVD-25 (G)	1.66	41.7	Amorphous	Separate and tilted columns
PVD-400/O_2^+	2.41	–	Anatase	Compact columns
PECVD (250)	2.19	11.8	Anatase	Compact columns made of crystallites
PECVD (25)	1.87	28.3	Amorphous	Compact columns
PECVD-1150(R)	Not available	–	Rutile	–

film interface [18] and their number and amplitude depend on the film refraction index and thickness. Thus, the larger the amplitude of the oscillations, the higher the value of the refraction index of the films. Refraction indices have been obtained from the analysis of the spectra in Fig. 4. The obtained values are reported in Table 1. According to the effective medium theories [19] the refraction index of a thin film of a given material depends on its pore volume and microstructure. As a first approximation, the lower the refraction index the larger the porosity. This general assessment is confirmed by the percentage of pore volume determined directly for some of the films by measuring their water adsorption isotherms with a QCM [17] (cf. Table 1). Extrapolation of this common trend to the films where no porosity data are available permits to conclude for example that sample PVD(G)-400 must be very porous, while sample PVD(O_2^+) must be very compact. This conclusion is confirmed by the observation of the microstructures of these two samples presented in Fig. 2. For the PECVD-1150 (R) thin film neither refraction index nor porosity data are available. Nevertheless, the observation by SEM of its surface topography suggests that its degree of compactness is similar to that of sample PECVD (250).

3.2. Degradation of dye molecules

To assess the photocatalytic activity we have measured the degradation rate of a solution of methyl orange in the presence of the illuminated thin films. The obtained results are reported in Fig. 5 for both the PVD and PECVD films. The plots show the evolution of the absorbance intensities of the methyl orange solution as a function of the illumination time. As references, curves corresponding to the

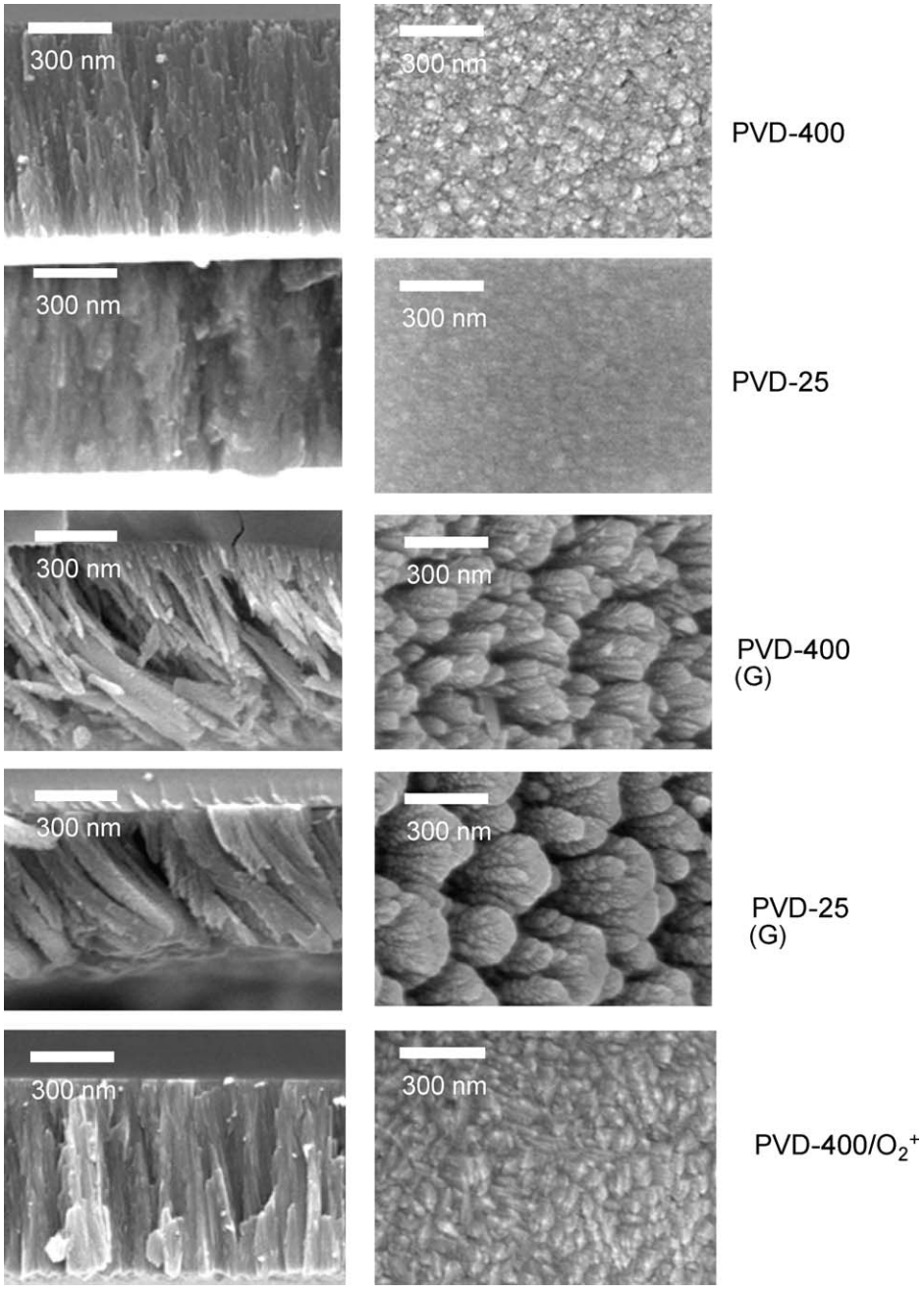

Fig. 2. Cross-section (left) and normal (right) views of TiO_2 thin films prepared by PVD.

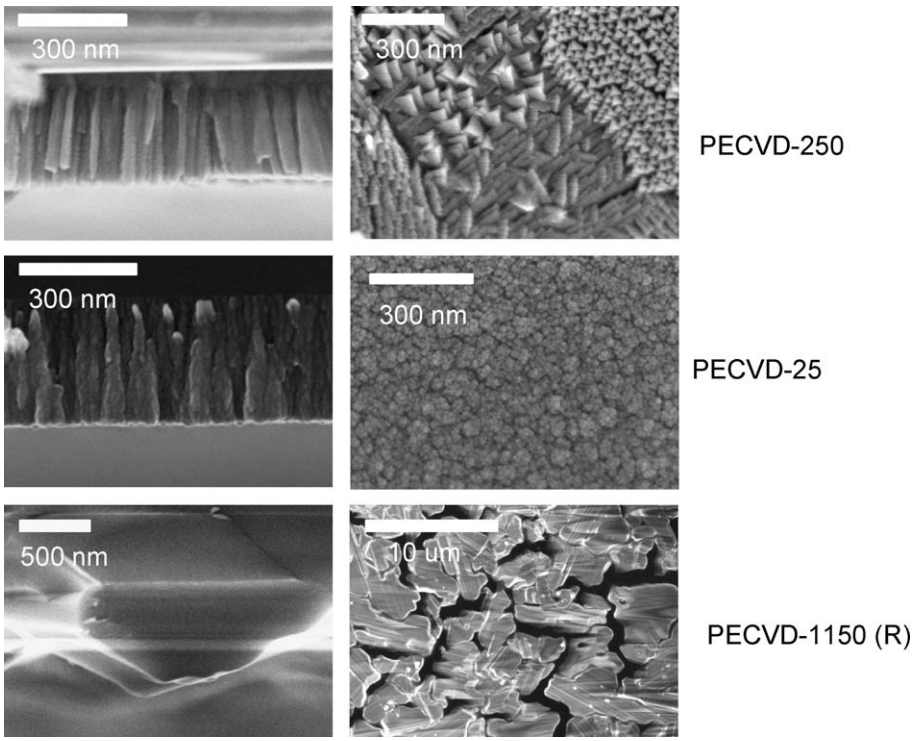

Fig. 3. Cross-section (left) and normal (right) views of TiO_2 thin films prepared by PECVD. The PECVD-1150 (R) film was prepared by annealing in air at 1150 °C sample PECVD-250.

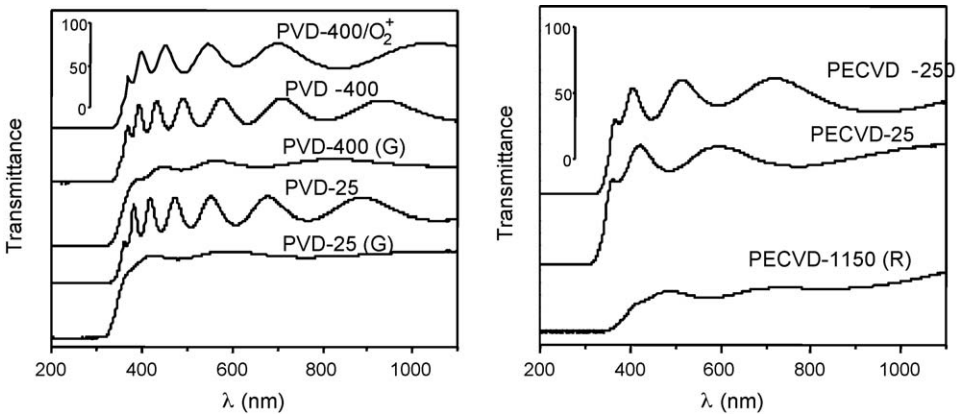

Fig. 4. UV–vis transmission spectra of TiO_2 thin films deposited on quartz plates by PVD (left) and PECVD (right). This latter also shows the spectrum of the PECVD-1150 (R) film. The spectra have been vertically displaced for clarity and the transmittance scales included in the two plots as insets.

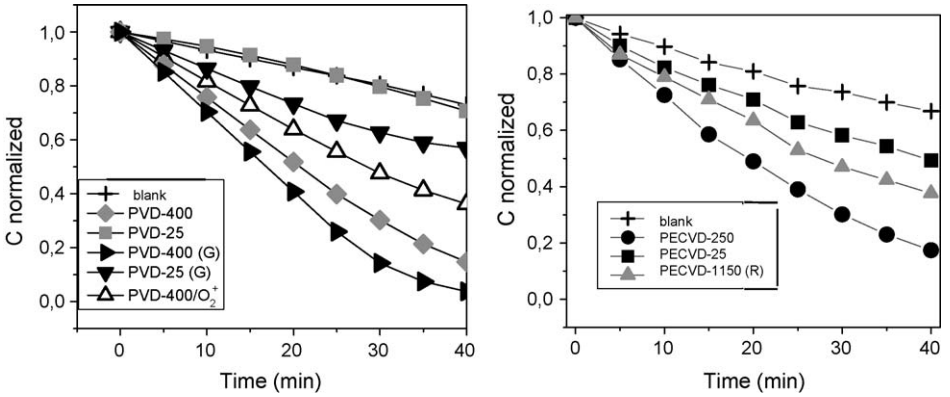

Fig. 5. Evolution of the normalized concentration of methyl orange in a water solution in the presence of illuminated TiO_2 thin films as indicated. (Left) PVD films and (right) PECVD and PECVD-1150 (R) films.

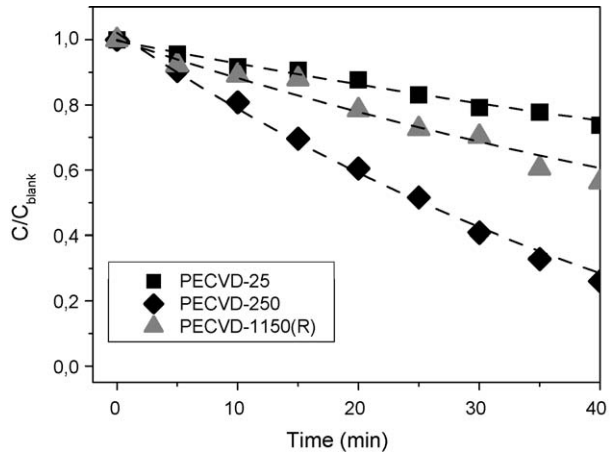

Fig. 6. Example of the experimental curves (symbols) accounting for the photo-catalytic degradation of the dye attributed to the thin films in the experiments of Fig. 5. The dashed lines correspond to the exponential curves used for fitting.

irradiation of the dye solutions without thin film are also reported. A first observation of the different curves clearly indicates that the most active film presents the anatase structure and a high porosity (e.g., sample PVD-400 (G)). This result is similar to the well established behaviour of TiO_2 powders where both the surface area and the anatase structure are the most important parameters for the determination of the their photo-catalytic activity [6,20,21].

From the curves plotted in Fig. 5, the actual photo-catalytic activities attributed to the films can be obtained by dividing their evolution curves by that of the blank test without film. Fig. 6 shows as examples two curves corresponding to the experiments carried out with the three PECVD films. For convenience we have adjusted these curves with exponentials functions of the type $\exp(-Kt)$ (i.e., a curve typical of a first-order kinetic, although this does not mean that this is actually the real kinetic of the process) as indicated by the dashed lines included in Fig. 6. An analysis similar to that depicted in Fig. 6 has been carried out for all the curves reported in Fig. 5. The values of the K constants obtained in this way are summarized in Table 2. At this point it is important to stress that although a proper fitting of the curves would likely require a more complex function, the choice of an exponential has the advantage of providing a single parameter (K) that can be used for a comparative assessment of the photo-activity of the different films. Note that a similar comparative analysis among the photo-activity of different samples would not be so straightforward with data obtained for TiO_2 in the form of powder where the agglomeration state of the sample may lead to substantial differences in the zone which actually is being illuminated.

Table 2
Values of the kinetics constants determined for the photo-catalytic degradation of dyes (K) and for the changes in the cosine of the wetting angles upon UV illumination (k_{UV}) and in the dark (k_{dark}).

Sample	K (min^{-1})	$-k_{UV}$ (min^{-1})[a]	k_{dark} (min^{-1})
PVD-400	3.0e−2	1.2	2.2e−2
PVD-25	0.0	1.3	2.5e−2
PVD-400 (G)	4.5e−2	3.2	2.9e−2
PVD-25 (G)	0.7e−2	2.9	5.7e−2
PVD-400/O_2^+	1.6e−2	1.2	6.4e−2
PECVD-250	3.0e−2	1.3	5.0e−2
PECVD-25	0.7e−2	1.2	1.4
PECVD-1150 (R)	1.3e−2	0.3	0.2

[a] $-k_{UV}$ indicates that the cosine of the wetting angle increases with the illumination time.

3.3. Wetting angle variation

The effect of the UV irradiation on the wetting angle on the films is reported in Fig. 7, where the value of this experimental parameter is represented against the irradiation time until reaching the superhydrophilic state (i.e., wetting angle smaller than 10°) and also for the recovery period when the samples are left in the dark. The behaviour in Fig. 7 is qualitatively similar to that reported in many previous works on this subject [2,4,5,22–24]. However, slight differences can be observed when looking in detail to the evolution of the wetting angle for the different thin films. A first difference stemming from the inset in Fig. 7 (left) is that the initial wetting angles are much smaller for the PVD thin films prepared at glancing angles (e.g., PVD (G) or PVD (G)-400 with wetting angles of 25° and 45°, respectively, the former already close to the value of 10° considered as threshold value of the superhydrophilic state). This fact, together with the rather equivalent kinetics found for the other films of this series, makes it difficult a straightforward comparison of the evolutions of their wetting angles under UV irradiation. Such an analysis can be done more properly by considering the evolution of the wetting angles on the PECVD films. The plots in Fig. 7 (right) clearly show that the kinetic of transformation follows the order PECVD-250 > PECVD-25 > PECVD-1150 (R). In contrast to this behaviour, the recovery in the dark of the original wetting angle is faster for sample PECVD-25 than for sample PECVD-250. Similarly, this recovery was much faster for samples PVD-25, PVD-400 and PVD-400-O_2^+ than for the two samples prepared at glancing angles.

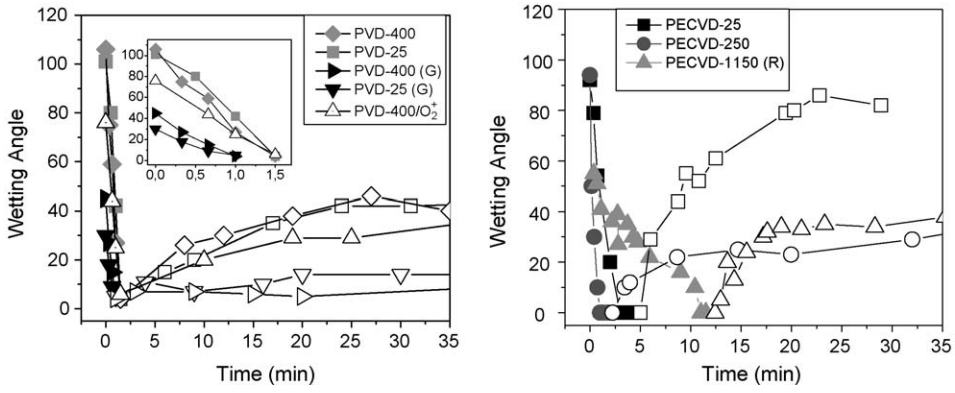

Fig. 7. Evolution of the wetting angle on illuminated PVD (left) and PECVD and PECVD-1150 (R) (right) thin films. The full symbols refer to the decay in wetting angle during illumination. The open symbols refer to the recovery of wetting angle when the illuminated thin films are kept in the dark. The inset shows an enlarged time scale the evolution of wetting angle for the PVD thin films under illumination.

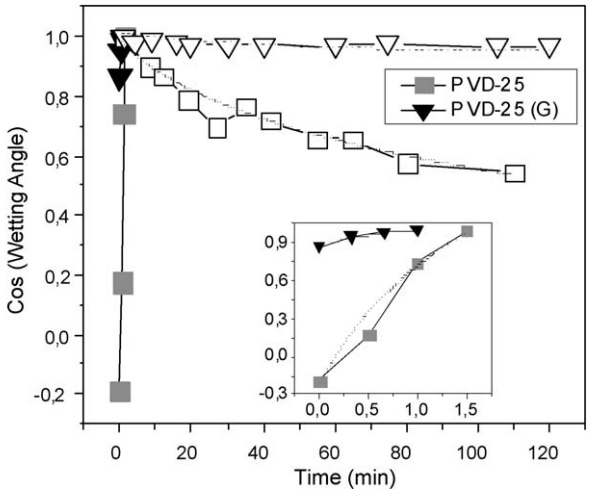

Fig. 8. Example of the representations of the evolution of the cosine of wetting angles and their fitting (dashed line) with two exponential functions, one for the samples under illumination (full symbols) and the other for the recovery in the dark (open symbols). The inset shows an enlarged time scale the evolution of wetting angle for the thin films under illumination.

Seki and Tachiya [25] have shown that the kinetic of the wetting angle decay upon UV irradiation and its recovery by keeping the films in the dark can be analysed by plotting the cosine of the wetting angle as a function of time. As examples Fig. 8 shows this evolution for thin films PVD-25 and PVD-25 (G), as well as fitting curves of the form $\exp(-k_{UV}t)$ and $\exp(-k_{dark}t)$, where $-k_{UV}$ and k_{dark} describe, respectively, the decay in wetting angle upon light irradiation and its posterior recovery in the dark. The obtained values for these constants for the whole series of films are reported in Table 2. The obtained values confirm the qualitative assessment made above based on the evolution of wetting angles depicted in Fig. 7. We stress again that the values of $-k_{UV}$ for the PVD films obtained at glancing angles are not very reliable and that therefore they must be considered with much caution in the discussion.

4. Discussion

The photocatalytic activity results presented in Fig. 6 and in Table 2, this latter in the form of pseudo-kinetic constants, clearly indicate that the anatase thin films are the most photo-catalytic active films and that for films of similar structure (i.e., anatase, rutile or amorphous) there is a direct correlation between the porosity and the efficiency for the UV degradation of dyes. In fact, according to the values of the K constants reported in Table 2 it is apparent that the photo-catalytic activity of the films follows the order: PVD-400 (G) > PVD-400 ≈ PECVD-250 > PVD-400/O_2^+ > PECVD-1150 (R) > PECVD-25 ≥ PVD-25 (G) > PVD-25 (0). The first sample of this series, PVD-400 (G), presents the anatase structure and a small value of refraction index (i.e., a very high porosity). Samples PVD-400 and PECVD-250 are both anatase and their refraction index are similar and higher than that of sample PVD-400 (G). In the previous ordering of photo-catalytic activities the film PVD-400/O_2^+ occupies a particular position since it presents much less activity than the other three anatase samples. This result must be related with its high refraction index value which is close to that of single crystalline anatase. This evidences that this film has practically no porosity and that, therefore, the active surface area exposed to the dye solution during the experiment is almost restricted to the its geometrical surface. Behind these four anatase thin films, the next most active material is the PECVD-1150 (R) thin film depicting the rutile structure. At the end of the series there appear the amorphous films that, although are characterized by a very small or nil photo-activity, are ordered inversely to the values of their refraction indices. Although for some dyes, differences in photo-catalytic degradation due to crystalline structures of films may be small, the significant differences found in our case among the anatase or amorphous films stress the importance of porosity in the overall photo-activity of thin films.

The previous results are in agreement to the current knowledge for powder materials where the anatase structure and the surface area of the powders are recognized as the most important factors to get an enhanced photo-catalytic activity [6,20,21]. A similar idea has been claimed to justify the use of columnar thin films prepared by evaporation at glancing angles for photo-voltaic cell applications [26].

In some works on the photo-catalytic activity of TiO_2 in the form of thin films it has been implicitly assumed that both wetting angle variation and photo-catalytic activity are related processes measuring the photo-activity of this material [2,4,5]. This assumption is not supported by the comparison of the K and $|-k_{UV}|$ values reported in Table 2. In fact, except for the PECVD-1150 (R) thin film and the two samples prepared at glancing angles where the reported values are rather uncertain, the other films present very similar k_{UV} values independently of their amorphous or anatase structures. This result is contradictory with the quite different photo-catalytic activities depicted by these thin films and suggests that the wetting angle transformation upon UV irradiation involves in a different manner the basic processes accounting for the photo-activity of TiO_2 (i.e., formation of e^-–h^+ pairs, their diffusion to the surface an their reaction with adsorbed species, primarily –OH^- groups [27]). Recently, working with single crystal materials, Yates et al. [28] have associated the decay in wetting angle upon UV irradiation with the photo-catalytic oxidation removal of organic contaminants always present on the surface of thin films. For the series of samples studied here, this would imply that the decay in wetting angle should be much faster for the anatase than for the amorphous films, the former presenting enhanced photo-catalytic activities. Since this is not observed, we must conclude that if the surface carbonaceous rests intervene in controlling the wetting angle variation, its importance must be negligible in our case.

On the other hand, the recovery of wetting angle when the superhydrophilic thin films are kept in the dark follows quite different kinetics. Thus, although the fastest process is presented by sample PECVD-25, the kinetics of the other films do not scale either with the type of crystal structure or with the porosity. Very likely other subtle surface effects related with the roughness, size of crystal domains or type of surface planes exposed at the surface must play a definite role in both the wetting angle decay upon UV irradiation and its recovery when the films are kept in the dark.

5. Conclusions

The previous results and discussion have shown that both the anatase structure and the porosity of the films are critical characteristics to increase their photo-catalytic activity. In this work we have also shown that a maximum activity for thin films prepared by PVD and PECVD correspond to samples PVD-400 (G) and PVD-400/PECVD-250, i.e., thin films prepared, respectively, by physical vapour deposition at a glancing angle and 400 °C as temperature of the substrate and by plasma deposition at 250 °C as substrate temperature.

On the other hand, the wetting angle variation depicts a more complex profile so that amorphous and crystalline films may present very similar kinetics. This result precludes a direct extrapolation of

photo-catalytic activity data to account for the superhydrophilic transformation of irradiated surfaces of TiO_2. Very likely, other factors like surface roughness, surface contamination, type of crystal planes at the surface, etc. must play a certain role in the UV-induced wetting behaviour of the films.

Acknowledgments

We thank the Spanish ministry for Science and innovation (project MAT2007-65764 and the CONSOLIDER project FUNCOAT), the Junta de Andalucía (project TEP2275) and the EU (project NATAMA 032583) for financial support.

References

[1] R. Wang, K. Hashimoto, A. Fujishima, M. Chikuni, E. Kojima, A. Kitamura, M. Shimohigoshi, T. Watanabe, Nature 388 (431) (1997) 431.
[2] T. Watanabe, A. Nakajima, R. Wang, M. Minabe, S. Koizumi, A. Fujishima, K. Hashimoto, Thin Solid Films 351 (1999) 260.
[3] O. Carp, C.L. Huisman, A. Reller, Prog. Solid State Chem. 32 (2004) 33.
[4] N.P. Mellott, C. Durucan, C.G. Pantano, M. Guglielmi, Thin Solid Films 502 (2006) 112.
[5] C.H. Kwon, J.H. Kim, I.S. Jung, H. Shin, K.H. Yoo, Ceram. Int. 29 (2003) 851.
[6] H. Arada, T. Ueda, Chem. Phys. Lett. 106 (1984) 229.
[7] I.A. Montoya, T. Viveros, J.M. Domínguez, L.A. Canales, I. Schifter, Catal. Lett. 15 (1992) 207.
[8] G. Degan, M. Tomkiewicz, J. Phys. Chem. 97 (1993) 12651.
[9] F. Gracia, J.P. Holgado, A.R. González-Elipe, Langmuir 20 (2004) 1688.
[10] A.P. Xagas, E. Androulaki, A. Hiskia, P. Falaras, Thin Solid Films 357 (1999) 173.
[11] A. Borrás, J. Cotrino, A.R. González-Elipe, J. Electrochem. Soc. 154 (2007) 152.
[12] R. Winter, D. Korzec, J. Engemann, Surf. Coat. Technol. 91 (1997) 101.
[13] A.C. van Popta, J. Cheng, J.C. Sit, M.J. Brett, J. Appl. Phys. 102 (2007) 013517.
[14] M.M. Hawkeye, M.J. Brett, J. Vac. Sci. Technol. A 25 (2007) 1317.
[15] A.R. González-Elipe, F. Yubero, J.M. Sanz, Low Energy Ion Assisted Film Growth, Imperial College Press, London, 2003.
[16] A. Garahan, L. Pilon, J. Yin, I. Saxena, J. Appl. Phys. 101 (2007) 014320.
[17] A. Borras, A. Barranco, A.R. Gonzalez-Elipe, J. Mater. Sci. 41 (2006) 5220.
[18] R. Swanepoel, J. Phys. E 16 (1983) 1213.
[19] F. Flory, L. Escoubas, Prog. Quant. Electron. 28 (2004) 89.
[20] J. Augustynski, Electrochim. Acta 38 (1993) 43.
[21] Sh. Ichikawa, R. Doi, Thin Solid Films 292 (1997) 130.
[22] M. Miyauchi, N. Kieda, Sh. Hishita, T. Mitsuhashi, A. Nakajima, T. Watanabe, K. Hashimoto, Surf. Sci. 511 (2002) 401.
[23] A. Nakajima, Sh. Koizumi, T. Watanabe, K. Hashimoto, J. Photochem. Photobiol. A: Chem. 146 (2001) 129.
[24] N. Stevens, C.I. Priest, R. Sedev, J. Ralston, Langmuir 19 (2003) 3272.
[25] K. Seki, M. Tachiya, J. Phys. Chem. 108 (2004) 4806.
[26] G.K. Kiema, M.J. Colgan, M.J. Brett, Sol. Energy Mater. Sol. Cells 85 (2005) 321.
[27] A.R. González-Elipe, G. Munera, J. Soria, J. Chem. Soc., Faraday I 75 (1979) 748.
[28] T. Zubkov, D. Stahl, T.L. Thompson, D. Panayotov, O. Diwald, J.T. Yates, J. Phys. Chem. B 109 (2005) 15454.